South East Asian J. of Mathematics and Mathematical Sciences
Vol. 20, No. 1 (2024), pp. 297-312

DOI: 10.56827/SEAJMMS.2024.2001.23 **ISSN (Online): 2582-0850**

ISSN (Print): 0972-7752

AGE-BASED INVESTIGATION OF COVID-19 PREVALENCE IN ETHIOPIA USING MATHEMATICAL MODELLING

Himani Agrawal, Atar Singh, Shyamsunder*, Harish Sharma and S. D. Purohit*****

Department of Mathematics,
Agra College, Dr. Bhim Rao Ambedkar University, Agra, INDIA

E-mail : himanigarg23.hg@gmail.com, atarsingh1968@gmail.com

*Department of Mathematics,
Malaviya National Institute of Technology Jaipur, INDIA

E-mail : skumawatmath@gmail.com

**Department of Computer Science and Engineering,
Rajasthan Technical University, Kota, INDIA

E-mail : hsharma@rtu.ac.in

***Department of HEAS (Mathematics),
Rajasthan Technical University, Kota, INDIA

E-mail : sunil_a_purohit@yahoo.com

(**Received:** *Jan. 06, 2024* **Accepted:** *Mar. 27, 2024* **Published:** *Apr. 30, 2024)*

Abstract: In December 2019, the newest infection, named novel coronavirus COVID-19, appeared, and it became a challenge to the world. In this paper, we investigated a mathematical model that explains the transmission of COVID-19 with the help of ordinary differential equations. Here, we divided the entire model into eight different compartments, namely $SEI_1I_2I_3QHR$ model based on three different age groups. Equilibrium analysis with positivity and boundedness are also investigated. The reproduction number is analyzed using Vandedressche's next-generation matrix. Stability analysis for disease-free equilibrium (DFE) is studied. We have taken some basic parameters with their primary conditions from the Ethiopian Ministry of Health Institute from 29 February 2021 to 07 June 2021.

Keywords and Phrases: COVID-19, Basic Reproduction Number, Stability Analysis.

2020 Mathematics Subject Classification: 92B05, 92D30, 34A34.

1. Introduction

Mathematical models are valuable tools widely recognized for helping us understand how diseases spread, both within individuals and across populations. Infection models provide insights into various aspects of epidemics, such as how infections progress in hosts and how infection transmitted among populations. Additionally, these models play a crucial role in formulating strategies to control diseases [14].

Currently, COVID-19 poses a significant global health challenge, affecting and claiming the lives of millions worldwide. It emerged in December 2019 in Wuhan, China, sparking a new outbreak of Coronavirus [26, 30]. By March 11, 2020, the World Health Organization (WHO) declared it a pandemic [28]. Common symptoms include fever, dry cough, and difficulty breathing, along with muscle pain, headaches, sore throat, and loss of taste or smell. To curb its spread, various measures like social distancing, wearing masks, frequent handwashing, minimizing non-essential travel, isolating cases, quarantining families, and closing schools and universities are being implemented [11, 17, 18, 23].

Ethiopia's Federal Ministry of Health (MOHE) and the Ethiopian Public Health Institute (EPHI) announced the first COVID-19 case in Addis Ababa on March 13, 2020. The initial patient was a 48-year-old Japanese traveler who had journeyed from Japan to Burkina Faso before reaching Addis Ababa [27]. According to MOHE and EPHI, anyone could contract COVID-19, but prompt action can help prevent its spread [1]. Employing all available intervention strategies is crucial for safeguarding our health and well-being. It's worth noting that older individuals and those with underlying health conditions, such as heart disease, respiratory ailments, or diabetes, face a higher risk of severe illness.

1.1. Literature Review

Medical reports indicate that both dengue and COVID-19 share similar symptoms during their early stages [20]. Scientists have analyzed and predicted the transmission patterns of these two deadly viruses in co-infection scenarios.

Agarwal et al. [2] developed a mathematical model to study the spread of COVID-19, focusing on how the virus transmits among individuals. This model calculates essential factors like the basic reproduction number to gauge COVID-19's transmissibility. Habenom et al. [13] created a mathematical model specifically tailored to analyze the transmission of COVID-19 in Ethiopia. This model helps

researchers understand how the virus behaves within the population.

Various mathematical models have been established to understand and predict the outbreaks of the COVID-19 pandemic, all based on the fundamental principles of population dynamics [6, 12, 19, 22]. Some studies have incorporated real-world data, including factors like isolation and quarantine, to enhance the accuracy of these models [4].

Chowdhury et al. [7] delved into the interaction between the immune system and the SARS-CoV-2 virus within infected individuals. Additionally, mathematical models have been developed to study the transmission processes of asymptomatic and symptomatic COVID-19 cases during outbreaks [8]. Youssef et al. [29] proposed an SEIR model using real data on COVID-19 spread in Saudi Arabia. Wang et al. [25] studied the adverse effects of isolation and quarantine during epidemics, particularly focusing on the social and emotional impacts. Russell et al. [21] analyzed travel data post-lockdown period (May-Sep.). Wang et al. [24] characterized a localized COVID-19 epidemic in Hubei province, China. Arhin et al. [3] developed a SEIRD model to predict COVID-19 trends in the USA.

Researchers have explored the spread of COVID-19 in various countries with different approaches using techniques like fuzzy clustering [16]. They've also investigated the stationary distribution of the pandemic and the likelihood of disease extinction using stochastic methods [9].

This study builds upon research conducted by Kumawat et al. [15], who investigated the transmission of COVID-19 using a mathematical model known as $SEI_1I_2I_3HR$. In this article, the authors adapt and expand upon this model to gain insights into how COVID-19 spreads in different age groups. They conduct numerical simulations as part of their investigation and present the findings visually through graphs. The findings from this study are expected to provide valuable information for understanding the disease dynamics and assessing the impact of quarantined populations in controlling its spread [10].

2. Model Formulation

The dynamic transmission of infectious disease is everywhere. Many researchers developed many mathematical models. Now we determined a mathematical model of an ordinary differential equation that can be determined an age factor is also a cause of the deadly disease of COVID-19. Here we divided the total human population into eight compartments, namely susceptible population $S(t)$, exposed population $E(t)$, and infected population is divided into three age groups namely I_1 (i.e., less than 14 years), I_2 (i.e., 15-54 years), I_3 (i.e., above 54 years), quarantined population $Q(t)$, hospitalized population $H(t)$ (clinically tested population), and removed population $R(t)$ (recovered or death) to formulate a mathematical model

$SEI_1I_2I_3QHR$. So, the total size of the population becomes $N(t) = S(t) + E(t) + I_1(t) + I_2(t) + I_3(t) + Q(t) + H(t) + R(t)$. Thus, the model is defined in Figure 1. All the individuals are assumed to be susceptible at a constant recruitment rate Δ. ν is the rate of susceptible individuals get infected with the force of infection $\nu = \frac{\kappa(I_1+\ell I_2+\wp I_3)}{N}$.

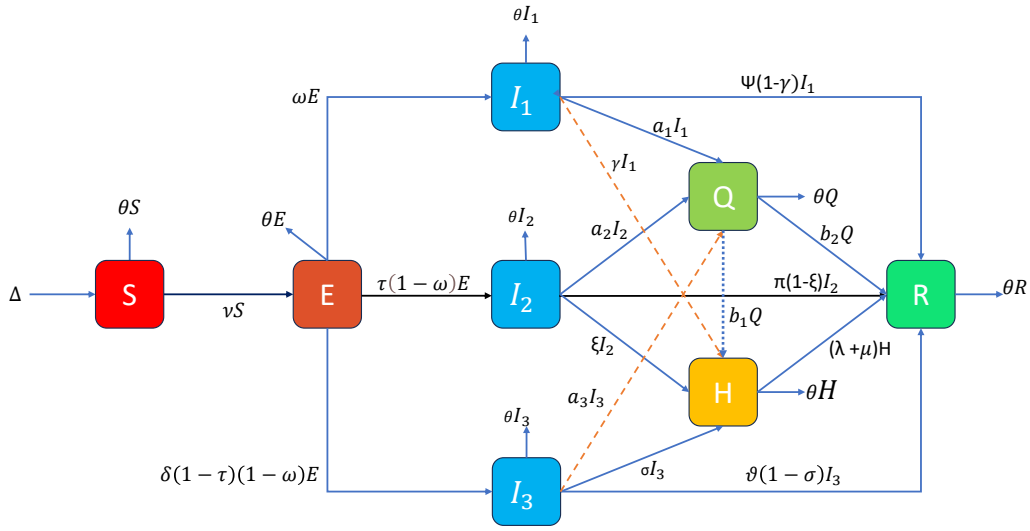

Figure 1: Diagram of $SEI_1I_2I_3QHR$ model.

$$
\begin{aligned}
\frac{ds}{dt} &= \Delta - (\nu + \theta)S, \\
\frac{dE}{dt} &= \nu S - \big(\omega + \tau(1-\omega) + \delta(1-\tau)(1-\omega) + \theta\big)E, \\
\frac{dI_1}{dt} &= \omega E - \big(\gamma + \psi(1-\gamma) + \theta + a_1\big)I_1, \\
\frac{dI_2}{dt} &= \tau(1-\omega)E - \big(\xi + \pi(1-\xi) + \theta + a_2\big)I_2, \\
\frac{dI_3}{dt} &= \delta(1-\tau)(1-\omega)E - \big(\sigma + \vartheta(1-\sigma) + \theta + a_3\big)I_3, \\
\frac{dQ}{dt} &= a_1I_1 + a_2I_2 + a_3I_3 - (b_1 + b_2 + \theta)Q,
\end{aligned}
\tag{1}
$$

$$\frac{dH}{dt} = \gamma I_1 + \xi I_2 + \sigma I_3 + b_1 Q - (\lambda + \mu + \theta)H,$$
$$\frac{dR}{dt} = \psi(1-\gamma)I_1 + \pi(1-\xi)I_2 + \vartheta(1-\sigma)I_3 + (\lambda+\mu)H + b_2 Q - \theta R.$$

With $S(0) \geq 0$, $E(0) \geq 0$, $I_1(0) \geq 0$, $I_2(0) \geq 0$, $I_3(0) \geq 0$, $Q(0) \geq 0$, $H(0) \geq 0$, $R(0) \geq 0$.

Table 1: Description of parameters in the model.

Parameters	**Interpretation**
μ	COVID-19 induces demise rate
θ	natural demise rate
ν	the rate of the susceptible population goes to exposed class
ω	the rate of the exposed population joining the infection the class I_1
τ	the rate of the exposed population joining the infection the class I_2
δ	the rate of the exposed population joining the infection the class I_3
γ	infected population of (0-14) years in hospital
ψ	the recovery rate of (0-14) years
ξ	the infected population of (15-54) years in hospital
π	recovery rate of (15-54) years
σ	infected population of (above 54) years in a hospital
ϑ	recovery rate of (above 54) years
λ	the rate of hospitalized population are recovered
κ	the rate of transmission or contact rate
ℓ	the mitigation factor for infected class I_2
$\wp$	the mitigation factor for infected class I_3
a_1	infected class I_1 goes to quarantined
a_2	infected class I_2 goes to quarantined
a_3	infected class I_3 goes to quarantined
b_1	the rate of quarantined class admit to hospital
b_2	the rate of quarantined class be recovered or death

3. Measure Resources of the Model

This section discusses the positivity and bounded properties of the proposed model 1. It introduces the following theorems to define the positivity of solutions and the physiologically invariant field.

Theorem 3.1. *Taking all the solution of the system with their starting values satisfy* $S(0) \geq 0$, $E(0) \geq 0$, $I_1(0) \geq 0$, $I_2(0) \geq 0$, $I_3(0) \geq 0$, $Q(0) \geq 0$, $H(0) \geq 0$, $R(0) \geq 0$, *then the solutions* $S(t)$, $E(t)$, $I_1(t)$, $I_2(t)$, $I_3(t)$, $Q(t)$, $H(t)$, $R(t)$

of the system (1) *are non-negative* $\forall\, t \geq 0$.

Proof. Take the model (1)'s first equation

$$\frac{dS(t)}{dt} = \Delta - (\nu + \theta)S(t),$$

$$\frac{dS(t)}{dt} \geq -(\nu + \theta)S(t),$$

by integration, we get

$$S(t) = S(0)\exp\big(-(\nu + \theta)t\big),$$

this gives

$$S(t) \geq 0.$$

Similarly $E(0) \geq 0, I_1(0) \geq 0, I_2(0) \geq 0, I_3(0) \geq 0, Q(0) \geq 0, H(0) \geq 0, R(0) \geq 0$. As a result, for any $t \geq 0$, the solution set $\{S(t),\ E(t),\ I_1(t),\ I_2(t),\ I_3(t),\ Q(t),\ H(t),\ R(t)\}$ of system (1) is non-negative.

Theorem 3.2. *With the initial conditions the solution of the system* (1) *which initiate in* $\mathbb{R}^8_+$ *are perfectly bounded in the positively invariant set* Ω.

Proof. The sum of all the equations in the model (1) yields the dynamics of the overall population, given by

$$\begin{aligned}
\frac{dN(t)}{dt} &= \frac{d}{dt}\big(S(t) + E(t) + I_1(t) + I_2(t) + I_3(t) + Q(t) + H(t) + R(t)\big),\\
\frac{dN(t)}{dt} &= \Delta - \theta\big(S(t) + E(t) + I_1(t) + I_2(t) + I_3(t) + Q(t) + H(t) + R(t)\big),\\
\frac{dN(t)}{dt} &= \Delta - \theta N(t).
\end{aligned}$$

Thus

$$\frac{dN}{dt} + \theta N(t) = \Delta.$$

The solution to the above equation is presented as follows

$$N(t) = \frac{\Delta}{\theta} - \Big(\frac{\Delta}{\theta} - N(0)\Big)\exp(-\theta t).$$

In accordance with the Birkhoff-Rota theorem [5], we get

$$0 \leq N(t) \leq \frac{\Delta}{\theta}, \quad t \to \infty.$$

Therefore, all possible solutions of model (1) converge in the domain
$\Omega = \left\{ S(t),\, E(t),\, I_1(t),\, I_2(t),\, I_3(t),\, Q(t),\, H(t),\, R(t) \in \mathbb{R}_+^8 : 0 \leq N(t) \leq \frac{\Delta}{\theta} \right\}.$

4. Equilibrium Analysis of $\mathbf{SEI_1I_2I_3QHR}$ Model

The DFE corresponds to the case in which the individual has no infections. All the infectious classes are set to zero. That is $E = I_1 = I_2 = I_3 = Q = H = 0$. Also, setting the derivatives of non-infectious classes to zero in Eq. (1) of our model. That is $\frac{dS}{dt} = \frac{dR}{dt} = 0$. Hence, the DFE point $\beth^0$ is given by

$$\beth^0 = \left(S^0,\, E^0,\, {I_1}^0,\, {I_2}^0,\, {I_3}^0,\, Q^0,\, H^0,\, R^0 \right) = \left(\frac{\Delta}{\theta},\, 0,\, 0,\, 0,\, 0,\, 0,\, 0,\, 0 \right). \tag{2}$$

The matrix F at $\beth^0$ given by

$$F = \begin{bmatrix} 0 & \kappa & \kappa\ell & \kappa\wp & 0 & 0 \\ 0 & 0 & 0 & 0 & 0 & 0 \\ 0 & 0 & 0 & 0 & 0 & 0 \\ 0 & 0 & 0 & 0 & 0 & 0 \\ 0 & 0 & 0 & 0 & 0 & 0 \\ 0 & 0 & 0 & 0 & 0 & 0 \end{bmatrix},$$

and the matrix V at $\beth^0$ is

$$V = \begin{bmatrix} M_1 & 0 & 0 & 0 & 0 & 0 \\ -\omega & M_2 & 0 & 0 & 0 & 0 \\ -\tau(1-\omega) & 0 & M_3 & 0 & 0 & 0 \\ -\delta(1-\tau)(1-\omega) & 0 & 0 & M_4 & 0 & 0 \\ 0 & -a_1 & -a_2 & -a_3 & 0 & b_1+b_2+\theta \\ 0 & -\gamma & -\xi & -\sigma & -b_1 & \lambda+\mu+\theta \end{bmatrix},$$

$$\begin{aligned} M_1 &= \omega + \tau(1-\omega) + \delta(1-\tau)(1-\omega) + \theta, \\ M_2 &= \gamma + \psi(1-\gamma) + \theta + a_1, \\ M_3 &= \xi + \pi(1-\xi) + \theta + a_2, \\ M_4 &= \sigma + \vartheta(1-\sigma) + \theta + a_3, \end{aligned}$$

then, the largest eigenvalue of the next generation matrix FV^{-1} is the required effective reproduction number which is define by

$$\mathcal{R}_0 = \frac{\kappa\omega}{M_1 M_2} + \frac{\kappa\ell\tau(1-\omega)}{M_1 M_3} + \frac{\kappa\wp\delta(1-\tau)(1-\omega)}{M_1 M_4}. \tag{3}$$

We get three effective reproduction numbers from Equation (3) for each age group.
$\mathcal{R}_{0I_1} = \frac{\kappa\omega}{M_1 M_2}$, for the effective individual for the age group (0-14) years,
$\mathcal{R}_{0I_2} = \frac{\kappa\ell\tau(1-\omega)}{M_1 M_3}$, for the effective individual for the age group (0-14) years,
$\mathcal{R}_{0I_3} = \frac{\kappa\wp\delta(1-\tau)(1-\omega)}{M_1 M_4}$, for the effective individual for the age group (0-14) years.
It can be written as a mathematical expression:

$$\mathcal{R}_0 = \mathcal{R}_{0I_1} + \mathcal{R}_{0I_2} + \mathcal{R}_{0I_3}.$$

Theorem 4.1. *The DFE point* $\beth^0\left(\frac{\Delta}{\theta}, 0, 0, 0, 0, 0, 0, 0\right)$ *is locally asymptotically stable for* $\mathcal{R}_0 < 1$*, otherwise unstable.*
Proof. To assess the local stability of the DFE point, we investigate the behavior of our model population near this equilibrium solution. At $\beth^0$, the Jacobian matrix of (1) is now:

$$J_{\beth^0} = \begin{bmatrix} -\theta & 0 & -\kappa & -\ell\kappa & -\wp\kappa & 0 & 0 & 0 \\ 0 & -M_1 & \kappa & \ell\kappa & \wp\kappa & 0 & 0 & 0 \\ 0 & \omega & -M_2 & 0 & 0 & 0 & 0 & 0 \\ 0 & \tau(1-\omega) & 0 & -M_3 & 0 & 0 & 0 & 0 \\ 0 & \delta(1-\tau)(1-\omega) & 0 & 0 & -M_4 & 0 & 0 & 0 \\ 0 & 0 & a_1 & a_2 & a_3 & -b_1-b_2-\theta & 0 & 0 \\ 0 & 0 & \gamma & \xi & \sigma & b_1 & -\lambda-\mu-\theta & 0 \\ 0 & 0 & \psi(1-\gamma) & \pi(1-\xi) & \vartheta(1-\sigma) & b_2 & \lambda+\mu & -\theta \end{bmatrix}.$$

The four eigenvalues are negative. i.e. $\alpha_1 = \alpha_2 = -\theta$, $\alpha_3 = -\lambda-\mu-\theta$, $\alpha_4 = -b_1-b_2-\theta$ and the following characteristic equation can be used to discover the remaining eigenvalues.

$$\alpha^4 + c_1\alpha^3 + c_2\alpha^2 + c_3\alpha + c_4 = 0,$$

where

$$\begin{aligned} c_1 &= M_1 + M_2 + M_3 + M_4, \\ c_2 &= M_2M_3 + M_2M_4 + M_3M_4 + M_1\big(M_2 + M_3 + M_4\big)\big(1-\mathcal{R}_0\big) \\ &\quad + (M_2+M_4)\,\frac{\kappa\ell\tau(1-\omega)}{M_3} + (M_2+M_3)\,\frac{\wp\kappa\delta(1-\tau)(1-\omega)}{M_4} + (M_3+M_4)\,\frac{\kappa\omega}{M_2}, \\ c_3 &= M_2M_3M_4 + M_1\left(M_3M_4 + M_2M_3 + M_2M_4\right)(1-\mathcal{R}_0) + \frac{M_3M_4\kappa\omega}{M_2} \\ &\quad + \frac{M_2M_4\kappa\ell\tau(1-\omega)}{M_3} + \frac{M_2M_3\wp\kappa\delta(1-\tau)(1-\omega)}{M_4}, \\ c_4 &= M_1M_2M_3M_4\,(1-\mathcal{R}_0)\,. \end{aligned}$$

In the above expressions we observe that the coefficient $c_1 > 0$, and the coefficients c_2, c_3 and c_4 are positive when $\mathcal{R}_0 < 1$. Moreover, the Routh-Hurwitz criteria for fourth-order polynomials are $c_i > 0,\ i = 1,\ 2,\ 3,\ 4, c_1c_2c_3 > {c_3}^2 + c_4{c_1}^2$ can be easily satisfied by applying the above coefficients. Thus, the model (1) at $\beth^0$ is locally asymptotically stable if $\mathcal{R}_0 < 1$ and unstable if $\mathcal{R}_0 > 1$.

5. Graphical Discussion and Result

Table 2: Parameter values used in model (1).

Parameter	Value (day^{-1})	Source	Parameter	Value (day^{-1})	Source
θ	0.0000404	[19]	γ	0.17970	[19]
κ	0.88960	[19]	ψ	0.15110	[19]
ω	0.00550	[19]	τ	0.02580	[19]
$\wp$	0.62880	[19]	μ	0.00016	[19]
ℓ	0.27010	[19]	ϑ	0.04320	[19]
ξ	0.10800	[19]	λ	0.03590	[19]
δ	0.02790	[19]	π	0.03880	[19]
σ	0.76350	[19]	Δ	4728.0	[19]
a_1	0.01020	Assumed	a_2	0.02300	Assumed
a_3	0.03201	Assumed	b_1	0.00280	Assumed
b_2	0.04000	Assumed			

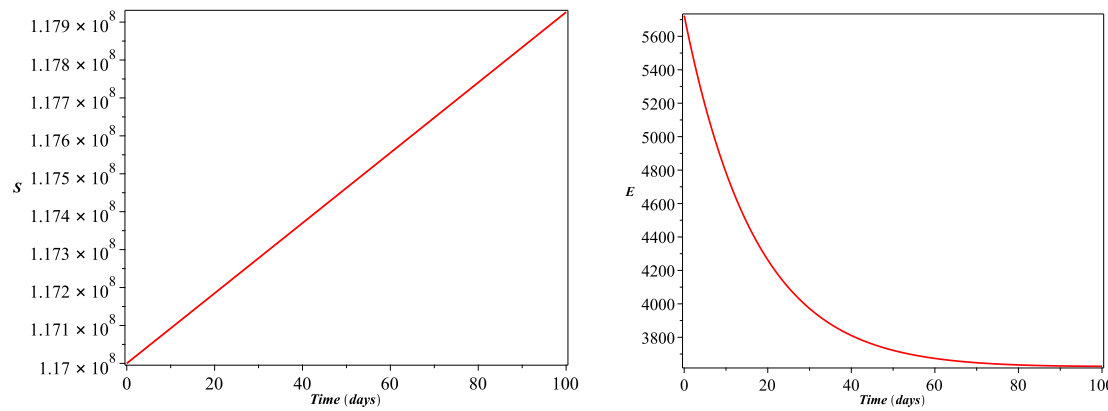

Figure 2: The dynamic behavior over time of (a) susceptible and (b) exposed populations.

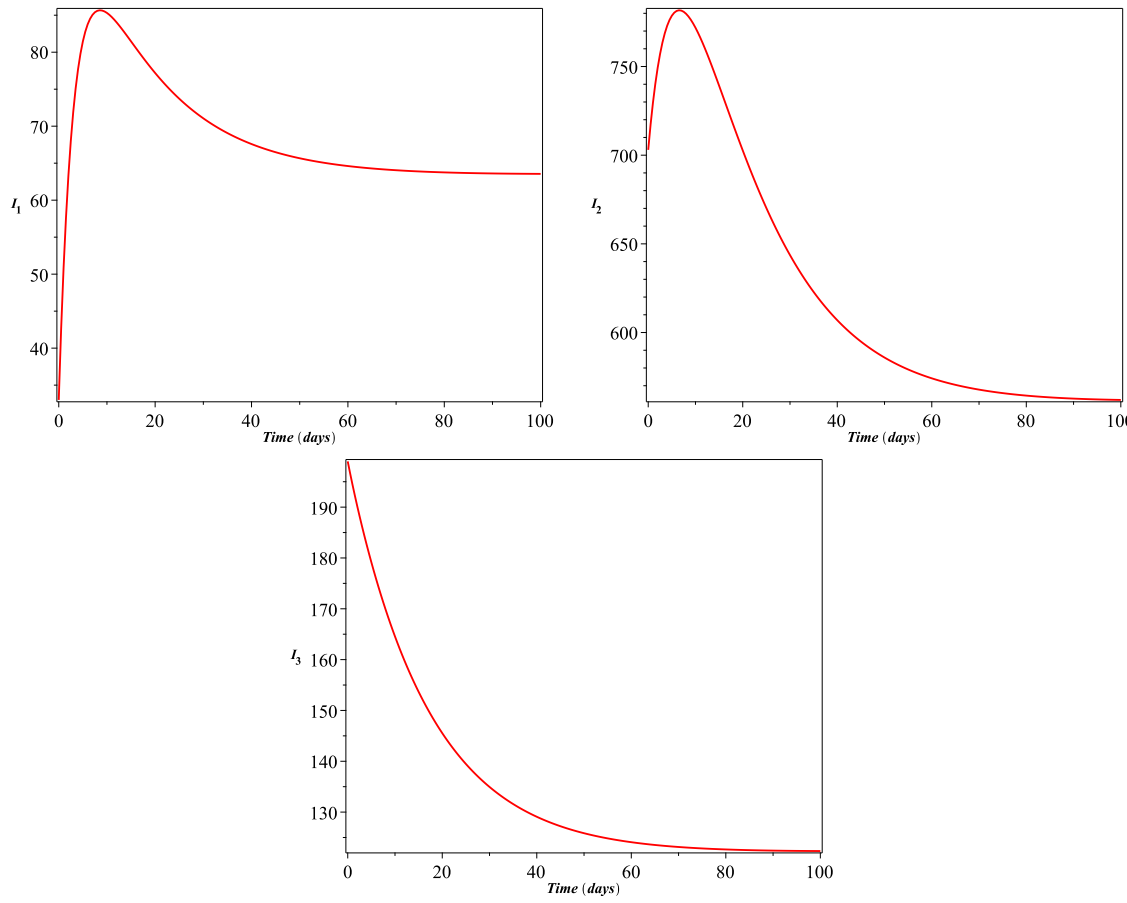

Figure 3: The dynamic behavior of the infected population over time is illustrated for (a) I_1, (b) I_2, and (c) I_3.

Numerical solutions for the $SEI_1I_2I_3HR$ model are derived using actual COVID-19 confirmed cases data from Ethiopia spanning 101 days, from February 28, 2021, to June 07, 2021 [1].

A numerical simulation is conducted based on the reported cases in Ethiopia, employing the following initial conditions for the system (1):

$S(0) = 1.17\times10^8,\ E(0) = 5724,\ I_1(0) = 33,\ I_2(0) = 703,\ I_3(0) = 199,\ Q(0) = 4200,\ H(0) = 20,144,\ R(0) = 954.$

The $SEI_1I_2I_3QHR$ model (1) is utilized as a age-based model for analyzing COVID-19 dynamics. We employ the ODE45 solver in MATLAB for graphical solution.

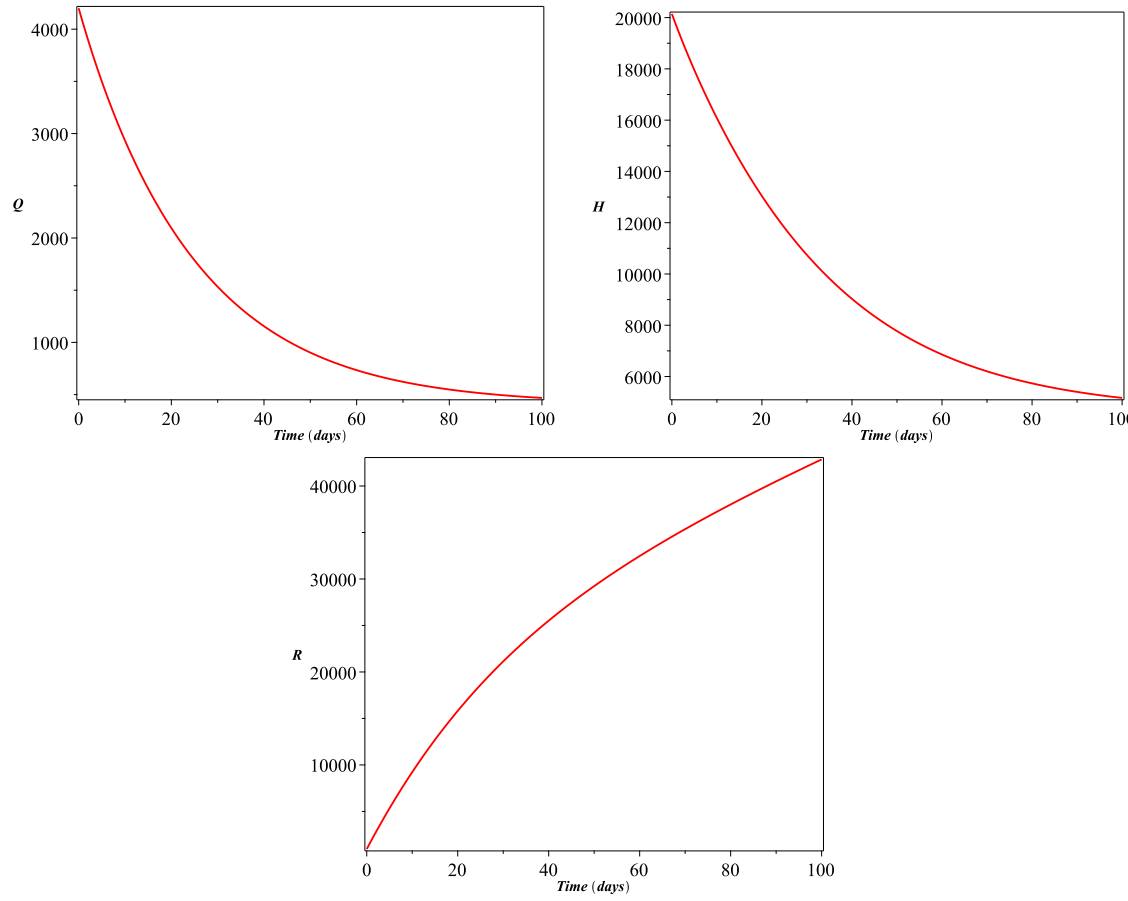

Figure 4: The dynamic behaviors over time of (a) quarantine, (b) hospitalization, and (c) recovered populations.

Figure 2(a) depicts a simulation of the susceptible population, showcasing its effective rate over time. Figure 2(b) depicts the dynamics of the exposed population, demonstrating a decline in the number of individuals exposed to the infection over time.

Meanwhile, Figures 3(a), (b), and (c) illustrate age-group-specific impacts over time.

Figure 4(a) showcases the dynamics of individuals in quarantine, providing insights into the efficacy of quarantine measures. Figure 4(b) shows the dynamic behavior of the population under treatment in a hospital or treatment center. Figure 4(c) offers insights into the recovery process, highlighting the trajectory of individuals who have successfully recovered from the infection.

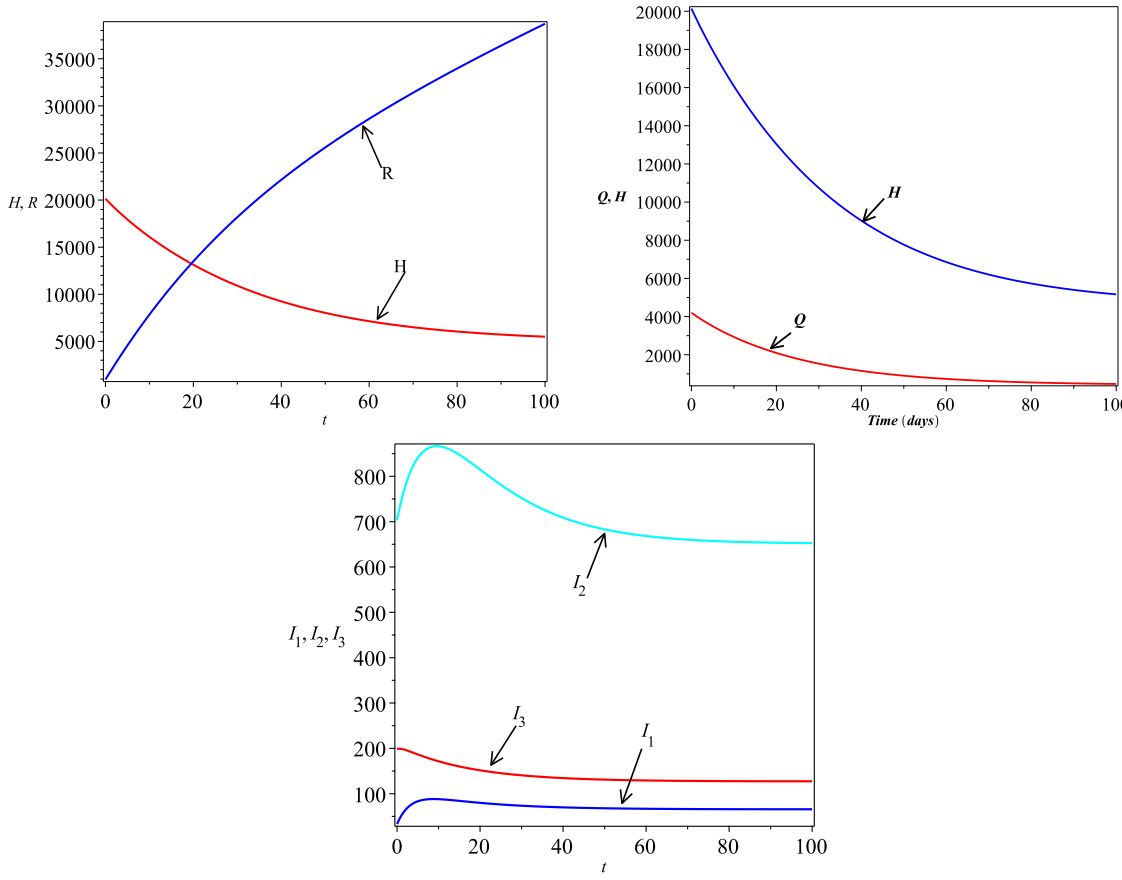

Figure 5: The behavior of the comparative solution of (a) H, R; (b) Q, H; and (c) I_1, I_2, I_3 over time.

Figure 5(a) offers a striking visual comparison between the trajectories of the recovered and hospitalized populations. Additionally, Figure 5(b) shows a comparison between the dynamics of quarantine and hospitalization. Figure 5(c) presents a comprehensive overview of the dynamic behavior of infections across all age groups, showing how infections behave over time in different age groups.

This analysis reveals that a reproduction number greater than one indicates the probability of the disease developing into an epidemic. In contrast, a value below one indicates the likelihood of the disease becoming extinct. Furthermore, it exhibits asymptotic stability. Transmission rates for each outcome are estimated by adjusting the parameters within different age groups. Conversely, changing the parameter's value also changes the resulting reproduction number. In short, a

reproduction number $\mathcal{R}_0 < 1$ indicates a rapid decline in the susceptible population within this simulation.

6. Conclusion

In this paper, we have investigated the spread of the COVID-19 disease using the $SEI_1I_2I_3QHR$ model. The proposed model has been solved using the MATLAB ODE45 solver. Our model's findings closely align with real-world data. The value of the basic reproductive number $\mathcal{R}_0 > 1$ indicates that one individual who tests positive for COVID-19 can lead to the infection of more than one new individual, signifying the ongoing spread of the coronavirus. Consequently, we recommend that everyone takes full responsibility for reducing the value of the basic reproductive number to below unity. Effective disease control hinges upon reducing virus transmission within the population. Throughout the pandemic, the Ethiopian government must take necessary steps to implement strategies aimed at reducing $\mathcal{R}_0$ through the manipulation of sensitive parameters.

Our study points to several important avenues for future research and action. First, active efforts should be made to bring the value of the basic reproduction number below unity, which indicates a significant reduction in transmission rates. This requires a comprehensive approach encompassing public health interventions, vaccination campaigns, and community engagement strategies. Furthermore, our findings underline the importance of continued monitoring and adaptation to emerging epidemiological trends. As the pandemic landscape changes, ongoing research efforts should focus on refining and updating models to capture emerging dynamics accurately. Finally, our study provides a basis for informed decision-making and underlines the importance of continued efforts in combating the COVID-19 pandemic. We can work toward a future with lower transmission rates and better public health outcomes by prioritizing ongoing research, collaboration, and proactive interventions.

Acknowledgments

The authors express their sincere thanks to the editor and reviewers for their fruitful comments and suggestions that improved the quality of the manuscript.

References

[1] Ministry of Health-Ethiopia and Ethiopian Public Health Institute, WHO characterizes COVID-19 as a pandemic, www.moh.gov.et and http://www.ephi.gov.et/.

[2] Agarwal, P., Ramadan, M. A., Rageh, A. A. and Hadhoud, A. R., A fractional-order mathematical model for analyzing the pandemic trend of COVID-19,

Math Methods Appl Sci, 45(8) (2022), 4625–4642.

[3] Arhin, J. R., Sam, F., Coker, K. and Ansah, E. O., An SEIRD epidemic model for predicting the spread of COVID-19 over a period of one year: A case of the united states, Am. J. Math. Comput. Model, 5(3) (2020), 70–76.

[4] Baleanu, D., Abadi, M. H., Jajarmi, A., Vahid, K. Z. and Nieto, J. J., A new comparative study on the general fractional model of COVID-19 with isolation and quarantine effects, Alex Eng J., 61(6) (2022), 4779–4791.

[5] Birkhoff, G. and Rota, G. C., Ordinary Differential Equations, Wiley: Hoboken, USA, 1989.

[6] Biswas, S. K., Ghosh, J. K., Sarkar, S. and Ghosh, U., COVID-19 pandemic in india: a mathematical model study, Nonlinear Dyn., 102(1) (2020), 537–553.

[7] Chowdhury, S. M. E. K., Chowdhury, J. T., Ahmed, S. F., Agarwal, P., Badruddin, I. A. and Kamangar, S., Mathematical modelling of COVID-19 disease dynamics: Interaction between immune system and SARS-CoV-2 within host, AIMS Math, 7(2) (2022a), 2618–2633.

[8] Chowdhury, S. M. E. K., Forkan, M., Ahmed, S. F., Agarwal, P., Ali, A. S. and Muyeen, S. M., Modeling the SARS-CoV-2 parallel transmission dynamics: asymptomatic and symptomatic pathways, Comput Biol Med, 143 (2022b), 105264.

[9] Din, A., Khan, A., and Baleanu, D., Stationary distribution and extinction of stochastic coronavirus (COVID-19) epidemic model, Chaos Solitons Fractals, 139 (2020), 110036.

[10] Dźiugys, A., Bieliùnas, M., Skarbalius, G., Misiulis, E., and Navakas, R., Simplified model of COVID-19 epidemic prognosis under quarantine and estimation of quarantine effectiveness, Chaos Solitons Fractals, 140 (2020), 110162.

[11] Disease Control, U. S. C. and (CDC), P. Coronavirus disease 2019 (covid-19): Prevention and treatment. Archived from the original on March 11, 2020, Retrieved March 11, 2020.

[12] Gumel, A. B., Iboi, E. A., Ngonghala, C. N. and Elbasha, E. H., A primer on using mathematics to understand COVID-19 dynamics: Modeling, analysis and simulations, Infect Dis Model, 6 (2021), 148–168.

[13] Habenom, H., Aychluh, M., Suthar, D. L., Al-Mdallal, Q. and Purohit, S. D., Modeling and analysis on the transmission of COVID-19 pandemic in Ethiopia, Alex. Eng. J., 61(7) (2022), 5323–5342.

[14] Kermack, W. O. and McKendrick, A. G., A contribution to the mathematical theory of epidemics, Proc R Soc. A, 115(772) (1927), 700–721.

[15] Kumawat, S., Bhatter, S., Suthar, D. L., Purohit, S. D. and Jangid, K., Numerical modeling on age-based study of coronavirus transmission, Appl. Math. Sci. Eng. (AMSE), 30(1) (2022), 609–634.

[16] Mahmoudi, M. R., Baleanu, D., Mansor, Z., Tuan, B. A. and Pho, K.-H., Fuzzy clustering method to compare the spread rate of COVID-19 in the high risks countries, Chaos Solitons Fractals, 140 (2020), 110230.

[17] Moore, S. E. and Okyere, E., Controlling the transmission dynamics of COVID-19, (2020), arXiv preprint arXiv:2004.00443.

[18] Mwalili, S., Kimathi, M., Ojiambo, V., Gathungu, D. and Mbogo, R., SEIR model for COVID-19 dynamics incorporating the environment and social distancing, BMC Notes, 13(1) (2020), 1–5.

[19] Okuonghae, D. and Omame, A., Analysis of a mathematical model for COVID-19 population dynamics in Lagos, Nigeria, Chaos Solitons Fractals, 139 (2020), 110032.

[20] Rehman, A. U., Singh, R. and Agarwal, P., Modeling, analysis and prediction of new variants of COVID-19 and dengue co-infection on complex network, Chaos Solitons Fractals, 150 (2021), 111008.

[21] Russell, T. W., Wu, J. T., Clifford, S., Edmunds, W. J., Kucharski, A. J. and Jit, M., Effect of internationally imported cases on internal spread of COVID-19: a mathematical modelling study, The Lancet Public Health, 6(1) (2021), e12–e20.

[22] Shyamsunder, Bhatter, S., Jangid, K., Abidemi, A., Owolabi, K. M. and Purohit, S. D., A new fractional mathematical model to study the impact of vaccination on COVID-19 outbreaks, Decision Analytics Journal, 6 (2023), 100156.

[23] U. S. Centers for Disease Control and Prevention (CDC), Coronavirus disease 2019 (COVID-19): Prevention and treatment, archived from the original on march 11, 2020, (2019).
https://www.who.int/emergencies/diseases/novel-coronavirus-2019/situation-reports. Retrieved March 11, 2020.

[24] Wang, C., Horby, P. W., Hayden, F. G. and Gao, G. F., A novel coronavirus outbreak of global health concern, The lancet, 395(10223) (2020), 470–473.

[25] Wang, Y., Shi, L., Que, J., Lu, Q., Liu, L., Lu, Z., Xu, Y., Liu, J., Sun, Y. and Meng, S., The impact of quarantine on mental health status among general population in China during the COVID-19 pandemic, Molecular psychiatry, 26(9) (2021), 4813–4822.

[26] World Health Organization, "advice for public.," archived from the original on 26 january 2020. Retrieved February 10 2020.

[27] World Health Organization, Ethiopia, the first case of COVID-19 confirmed in Ethiopia.
https://www.afro.who.int/news/first-Marchcase-covid-19-confirmed-ethiopia.

[28] World Health Organization, WHO characterizes COVID-19 as a pandemic.
https://www.who.int/emergencies/diseases/novel-coronavirus-2019/situation-reports.

[29] Youssef, H. M., Alghamdi, N. A., Ezzat, M. A., El-Bary, A. A. and Shawky, A. M., A new dynamical modeling SEIR with global analysis applied to the real data of spreading COVID-19 in Saudi Arabia, Math. Biosci. Eng, 17(6) (2020), 7018–7044.

[30] Zhu, H., Wei, L. and Niu, P., The novel coronavirus outbreak in Wuhan, China. Global health research and policy, 5(6) (2020), 1–3.